運輸省港湾技術研究所

港湾技術研究所報告

REPORT OF THE PORT AND HARBOUR RESEARCH INSTITUTE

MINISTRY OF TRANSPORT

VOL. 13 NO. 4 DEC. 1974

NAGASE, YOKOSUKA, JAPAN

港湾技術研究所報告 (REPORT OF P.H.R.I.)

第13巻 第4号 (Vol. 13, No. 4), 1974年12月 (Dec. 1974)

目 次 (CONTENTS)

REPORT OF THE PORT AND
HARBOUR RESEARCH INSTITUTE
Vol. 13 No. 4 (Dec. 1974)

Calculation of the Wave Speed for a Logarithmic Drift Current

Hajime KATO*

Synopsis

In this paper an attempt is made to estimate as accurately as possible the effect of drift current on the wave speed. First, a modified logarithmic velocity distribution is proposed, which applys well to the observed drift current profiles. Then, by using the perturbation method the phase speed of small amplitude waves for the proposed logarithmic profile is calculated to the second-order in the form

$$c=c_0\left[1+\varepsilon\frac{c_1}{c_0}+\varepsilon^2\frac{c_2}{c_0}\right],\quad \varepsilon=u_0/c_0$$

where u_0 is the surface velocity, c_0 the wave speed for no current.

From the numerical computations the second-order term is found to be very small even when the parameter ε is relatively large. In this connection the validity of the present perturbation method is discussed shortly. It is also found that the modification of the velocity profile near the bottom for a return flow has little effect on the wave speed, while the present logarithmic profile gives fairly smaller wave speeds than the parabolic profile which was assumed previously. This indicates that the form of the drift current profile close to the water surface is very important in determining the wave speeds. In the calculation several special functions appear and the behaviors of those are inquired into briefly.

* Chief of the Hydrodynamics Laboratory, Marine Hydrodynamics Division

港湾技術研究所報告
第13巻 第4号 (1974.12)

対数分布の吹送流に対する波速の計算

加 藤 始*

要 旨

この報告では，吹送流が波速におよぼす影響をできるだけ正確に求めることが試みられている。まず実際の吹送流の分布にもよくあてはまり，計算にも都合のよい対数分布を導入する。その速度分布をもつ流れの中の微小振幅波の波速をせつ動法により第2次近似まで計算するが，結果は次の形で表わされる。

$$c=c_0\left[1+\varepsilon\frac{c_1}{c_0}+\varepsilon^2\frac{c_2}{c_0}\right],\quad \varepsilon=u_0/c_0$$

ここに u_0 は表面流速，c_0 は流れのないときの波速で，c_1/c_0，c_2/c_0 は u_0 に無関係に求められる。

実験室でみられる吹送流においては，パラメータ ε はあまり小さくならない。しかし，今回の数値計算の結果では，前に計算した放物線分布の場合と同様に，ε があまり小さくなくても第2次近似の項は非常に小さいことが見出される。これに関連して，この種のせつ動法の妥当性についてもふれられる。また今回の対数分布について求められた波速は，前の放物線分布に対する波速よりもかなり小さいことがわかったが，一方，実験室での反流に対応して底面近くの流速分布を変化させても，えられる波速には大した差は出ないことが示される。このことは，波速の計算のためには水面のすぐ近くでの吹送流分布の正確さが重要であることを示している。

なお，数値計算のためには Shi x，Chi x その他の特殊な関数が現われるが，それらの値や性質も簡単に示される。

* 海洋水理部 水理研究室長

CONTENTS

1. Introduction

It has been found by many investigators that the phase velocity of wind-generated waves is appreciably larger than the wave speed in the still water c_0 calculated from the linear wave theory. The difference is much larger than the finite-amplitude effect and has mainly been attributed to the effect of drift current.

Lilly[1] presented a perturbation procedure for obtaining wave speed solutions for drift-type flows with the surface velocity u_0 much smaller than the wave speed c_0. Hidy & Plate (1966) used Lilly's first-order solution for a laminar parabolic profile with zero net transport for correcting the observed phase velocities of dominant waves. However, for an actual drift current in the laboratory the ratio of surface velocity to wave speed u_0/c_0 is not very small and the velocity profile is much different from the laminar parabolic profile. By using a perturbation method similar to Lilly, Kato (1972) calculated the wave speed to the second order for a different parabolic drift profile which exists only in near surface layer, and showed that the second order solution is negligible even when the perturbation parameter u_0/c_0 is relatively large. Since it was rather unexpected result, the numerical values of wave speed from perturbation solutions were compared with the numerical solutions obtained by the method of series expansion, and the two agreed surprisingly well.

Recently it has been reported by both Shemdin (1972) and Dobroklonsky & Lesnikov (1972) that the observed drift current profiles are logarithmic. Shemdin also investigated the influence of wind on wave speeds by solving a boundary value problem of the coupled shear flows in air and water, although his method was not effective in obtaining a numerical solution for the experimental wave condition in the wavelength range 12.9~126 cm.

The effects of adverse wind on the wave speed have been studied theoretically as well as experimentally by Mizuno & Mitsuyasu (1973a, b). The wave speeds were calculated by considering both effects of drift current with the parabolic profile which was identical with Kato (1972) and of wave-induced aerodynamic pressure, and it was suggested that some discrepancy between theoretical and experimental results might have been attributed to the rough approximation of the assumed current profile. A logarithmic drift current profile has been confirmed also in our measurements (Kato & Tsuruya (1974)).

The phase velocities of actually observed waves are influenced not only by the drift current and aerodynamic effect but also by other factors such as directional spreading of waves, fluctuations of drift current, effect of harmonic components, etc. Since, however, a drift current undoubtedly causes a major effect on the wave speed, it would not be worthless to calculate only the effect of drift current on the wave speed as accurately as possible.

In this report is described a calculation of the wave speed for the case where linear waves propagate on a logarithmic drift current under no wind. Although a second order solution was of little significance for the previous parabolic drift, since the logarithmic profile is different from the former one and the values of u_0/c_0 which we expect are relatively large, the calculation is extended to the second order again by using the perturbation method after Lilly[1].

2. The profile of drift current

Concerning the drift current, measurements of the surface velocity u_0 have so far been made by many investigators. It was found by Keulegan (1951) that the surface velocity is not affected by the presence of the waves and that the ratio of u_0 to the average wind velocity V tends to a constant value of about 0.033 at high Reynolds numbers $u_0 d/\nu$, where d is the liquid depth, ν the kinematic viscosity. Using the free stream (or maximum) wind velocity V_∞, Keulegan's limiting value was equivalent to $u_0/V_\infty=0.030$, and the ratio found by Plate *et al* (1969) was $u_0/V_\infty=0.026$. Wu (1968) used small float of various sizes to determine the drift current in near surface layer and obtained much higher surface velocity than those reported elsewhere; $u_0/V_\infty=0.048$ at $V_\infty=8.40$ m/sec. Wu claimed that the difference was due to the superiority of his method. In our laboratory also the measurements of drift current have been and are being made by means of various methods, some of which are reported by Kato & Tsuruya (1974). The ratios u_0/V_∞ so far obtained are always about 0.028 at sufficiently high Reynolds numbers.

The measurement of the drift current profile is not easy and no complete data had been reported except Baines & Knapp (1965) who made measurements by inhibiting the formation of waves with detergent. Recently it was found by Shemdin (1972) and Dobroklonsky & Lesnikov (1972) that the observed velocity distributions of drift current are expressed in the form

$$U(z)=B_1-A_1 \ln z\,, \qquad (2.1)$$

where z is the depth from the water surface, and B_1 and A_1 are arbitrary constants. Shemdin proposed a logarithmic profile of the form

$$u_0-U(z)=A_1 \ln (z/z_{0_w})\,, \qquad (2.2)$$

where z_{0_w} is a roughness height. The above relation, whether (2.1) or (2.2) fails to be valid close to the surface $z=0$. Actually it is believed that a small viscous layer exists immediately below the surface and the velocity gradient is constant there. The drift current velocities down to the depth $z=3.8$ mm obtained by Wu (1968) exhibit linear changes with depth. On the other hand, the drift profiles obtained by Dobroklonsky & Lesnikov (1972), one of which (Case I) is shown in Fig. 1, indicate that the thickness of the viscous layer, if any, is much smaller than 1 mm. According to Banner & Phillips (1973) the thickness of this layer must be proportional to $\nu(\rho/\tau_0)^{1/2}$, where ρ is the water density and τ_0 the mean tangential wind stress at the surface.

Aside from the physical mechanism, for the use in calculating the wave speed we assume the drift current profile in near surface layer of the form

$$U(y)=u_0-U_r \ln\left(\frac{z_0-y}{z_0}\right), \qquad (2.3)$$

where y is measured upward from the water surface, u_0 is the surface drift velocity, U_r and z_0 are arbitrary constants which are to be determined corresponding to the actual drift profile.

Fig. 2 shows the drift profiles obtained by Kato & Tsuruya (1974) by means of a hot-film anemometer and suppressing waves with detergent. It is seen from

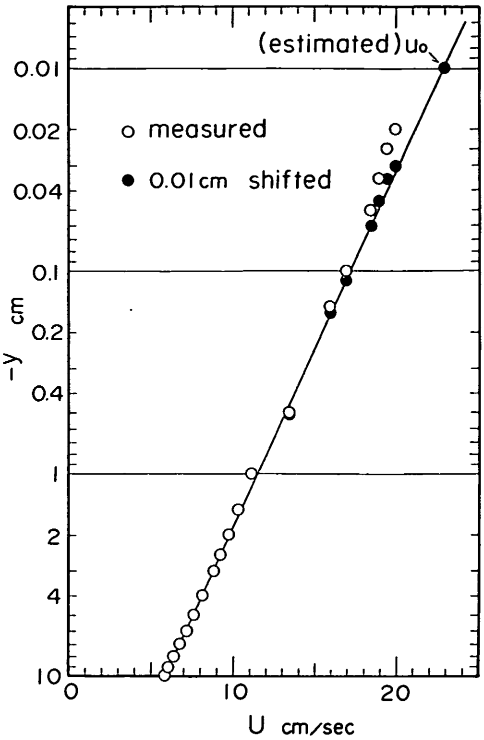

Fig. 1. Drift current profile (from Dobroklonsky & Lesnikov[4]).

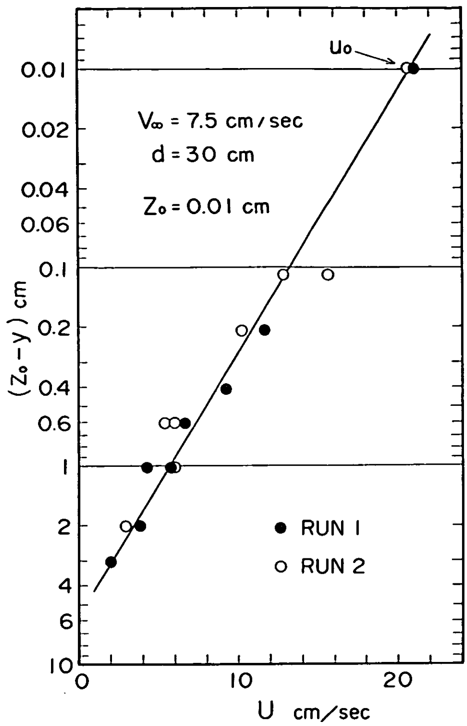

Fig. 2. Drift current profile (from Kato & Tsuruya[7]).

this figure that the measured profiles can be expressed to a good approximation as (2.3) by putting roughly $z_0=0.01$ cm, although more data are necessary for determination of the most suitable value of z_0. Dobroklonsky & Lesnikov (1972) reported nothing about the surface drift velocity u_0. But if we shift all the measurement depths by 0.01 cm in order to apply (2.3) to their data, the shifted points are aligned on a straight line as shown with solid dots in Fig. 1. Then we obtain the estimated value of $u_0 \fallingdotseq 23$ cm/sec from a point on the line corresponding to the surface ($y=0$). Since the free stream wind velocity for this case seems to be about 8.5 m/sec, we can estimate $u_0/V_\infty=0.027$ which is in agreement with the results obtained so far. Even if the real value of u_0 differs somewhat from 23 cm/sec, it will be possible to apply (2.3) to the data as well by adjusting the value of z_0. It thus appears that we may use (2.3) as an approximate equation for the real drift current profile near the water surface.

On the other hand, a return flow is usually induced in a wind-wave channel and so a drift current profile deviates from the distribution (2.3) with increasing depth. In such a case it might be possible to use the distribution

$$U(y)=u_0-U_r\ln\left(\frac{z_0-y}{z_0}\right)-by\,, \tag{2.4}$$

in place of (2.3) on the assumption that the constant b is sufficiently small. Considering zero net transport in horizontal direction, the condition

$$\int_{-d}^{0} U(y)dy=0\,, \tag{2.5}$$

must be satisfied.

In our experiments the distribution of return flow was found to be nearly uniform.[7] If we add the condition

$$U(-d)=U\left(-\frac{d}{2}\right), \tag{2.6}$$

neglecting the bottom boundary layer, then U_r and b are given by

$$U_r=u_0\Big/\left\{\left(1+\frac{z_0}{d}\right)\ln\left(\frac{d+z_0}{z_0}\right)-\ln\left(\frac{d+z_0}{d/2+z_0}\right)-1\right\}, \tag{2.7}$$

$$b=\frac{2}{d}U_r\ln\left(\frac{d+z_0}{d/2+z_0}\right). \tag{2.8}$$

Two examples of the distribution (2.4) for $d=50$ cm and $u_0=28$ cm/sec which satisfys the conditions (2.5) and (2.6) are shown together with those of (2.3) in Fig. 3, and the corresponding values of z_0, U_r, b and bd are listed in Table 1. Since the value of b is fairly small as seen from Table 1 and the difference between (2.3) and (2.4) at the depth $y/d=-0.1$ is 0.5 to 0.7 cm/sec, we can practically use the approximation (2.4). Actually it will be shown later that the difference between the wave speeds calculated for (2.3) and (2.4) is very small.

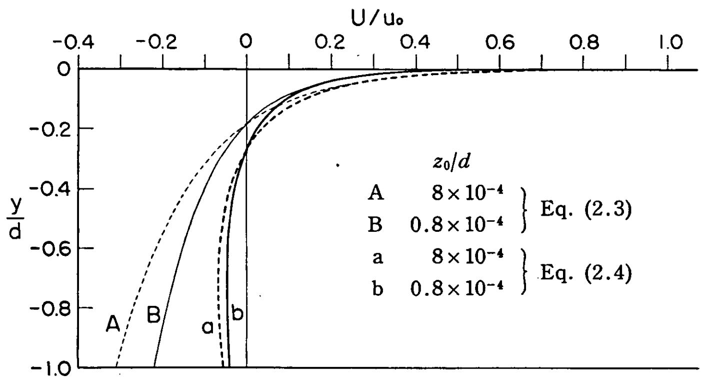

Fig. 3. Logarithmic distributions of Eqs. (2.3) and (2.4).

Table 1 Data relevant to Fig. 3

($u_0=28.0$ cm/sec, $d=50$ cm)

Profile	z_0/d	z_0 (cm)	U_r (cm/sec)	b (sec^{-1})	bd (cm/sec)
A	8.0×10^{-4}	0.04	5.1423	0	0
B	8.0×10^{-5}	0.004	3.6170	0	0
a	8.0×10^{-4}	0.04	5.1423	0.14241	7.121
b	8.0×10^{-5}	0.004	3.6170	0.10027	5.014
c*	2.0×10^{-4}	0.01	4.1019	0.11370	5.684

(* Profile-c is not shown in Fig. 3)

3. Calculation of wave speed for a logarithmic current profile

Although the velocity distribution which we originally aimed to deal with is Eq. (2.3), for the calculation in this section we use Eq. (2.4), namely

$$U(y)=u_0-U_r\ln\left(\frac{z_0-y}{z_0}\right)-by\,, \tag{3.1}$$

so that we can apply the results immediately to the drift current with a return flow as stated in the foregoing section. The solution for the case of profile (2.3) will be obtained simply by putting $b=0$ in the final results.

We shall consider small disturbances on a current whose velocity distribution is given by (3.1), where y is measured upward from the water surface as before. The entire motion will be regarded as two-dimensional, the x-axis being taken to coincide with the direction of the current. Let the x- and y-components of velocity due to the wave motion be u and v, respectively. If the turbulent velocity fluctuations are neglected, then the linearized equations of motion are

$$\left.\begin{aligned}\frac{\partial u}{\partial t}+U\frac{\partial u}{\partial x}+v\frac{\partial U}{\partial y}&=-\frac{1}{\rho}\frac{\partial p}{\partial x}\,,\\ \frac{\partial v}{\partial t}+U\frac{\partial v}{\partial x}&=-\frac{1}{\rho}\frac{\partial p}{\partial y}-g\,,\end{aligned}\right\} \tag{3.2a, b}$$

$$\frac{\partial u}{\partial x}+\frac{\partial v}{\partial y}=0\,, \tag{3.3}$$

where p is the disturbance pressure, g the acceleration of gravity, and ρ the constant water density. The boundary conditions on the free surface $y=\eta(x, t)$ are

$$\frac{\partial \eta}{\partial t}+U\frac{\partial \eta}{\partial x}=v\,,\quad (\text{at } y=\eta) \tag{3.4}$$

$$p+\sigma\frac{\partial^2 \eta}{\partial x^2}=0\,,\qquad (\text{at } y=\eta) \tag{3.5}$$

where σ is the surface tension. The bottom condition is

$$v=0\,.\qquad (\text{at } y=-d) \tag{3.6}$$

The wave motion may be characterized by a stream function $\psi(x, y)$ such that

$$u=-\frac{\partial \psi}{\partial y}\quad\text{and}\quad v=\frac{\partial \psi}{\partial x} \tag{3.7a, b}$$

which satisfy the continuity equation (3.3). Upon eliminating the pressure between (3.2a) and (3.2b), the following equation is obtained

$$\left(\frac{\partial}{\partial t}+U\frac{\partial}{\partial x}\right)\nabla^2\psi-\frac{\partial^2 U}{\partial y^2}\frac{\partial \psi}{\partial x}=0\,. \tag{3.8}$$

The solution of (3.8) may be assumed to have the form

$$\psi=\phi(y)e^{ik(x-ct)} \tag{3.9}$$

which represents a simple harmonic wave of permanent form

$$\eta=ae^{ik(x-ct)} \tag{3.10}$$

where c is a constant wave speed and k the wavenumber. Substituting (3.9) in Eq. (3.8), the following equation for ϕ is found

$$(U-c)(\phi''-k^2\phi)-U''\phi=0\,, \tag{3.11}$$

where the primes indicate differentiation with respect to y. If we use the expression for p such that

$$p=\rho[(U-c)\phi'-\phi U']e^{ik(x-ct)}-\rho gy\,, \tag{3.12}$$

then, the surface boundary condition for ϕ is obtained, from (3.4) and (3.5) in the form

$$(U-c)[(U-c)\phi'-\phi U']=\left(g+\frac{\sigma k^2}{\rho}\right)\phi. \quad (y=0) \tag{3.13}$$

The bottom condition (3.6) becomes

$$\phi=0\,. \quad (y=-d) \tag{3.14}$$

The wave speed c will be obtained by solving Eq. (3.11) with the conditions (3.13) and (3.14). We use the perturbation method after Lilly[1] in which u_0/c_0 is taken as a parameter, seeking the solution to the second order. Hence, we put

$$\phi=\phi_0+\varepsilon\phi_1+\varepsilon^2\phi_2+\cdots, \tag{3.15}$$

$$c=c_0+\varepsilon c_1+\varepsilon^2 c_2+\cdots, \tag{3.16}$$

where $\varepsilon=u_0/c_0$ is assumed to be a small parameter. Substituting (3.15) and (3.16) in (3.11) and equating terms of the same power of ε, by considering U/u_0 to be of the order of ε, the following equations are obtained:

$$\left.\begin{aligned}
&\phi_0''-k^2\phi_0=0\,,\\
&\phi_1''-k^2\phi_1=-\left(\frac{U''}{u_0}\right)\phi_0\,,\\
&\phi_2''-k^2\phi_2=-\left(\frac{U''}{u_0}\right)\phi_0\left(\frac{U}{u_0}-\frac{c_1}{c_0}\right)-\frac{U''}{u_0}\phi_1\,.
\end{aligned}\right\} \tag{3.17a, b, c}$$

The boundary condition (3.13) at $y=0$ is similarly reduced to

$$\left.\begin{aligned}
&\phi_0'-(g_r/c_0^2)\phi_0=0\,, \quad (y=0)\\
&\phi_1'-(g_r/c_0^2)\phi_1=2\left(\frac{U}{u_0}-\frac{c_1}{c_0}\right)\phi_0'-\frac{U'}{u_0}\phi_0\,, \quad (y=0)\\
&\phi_2'-(g_r/c_0^2)\phi_2=2\left(\frac{U}{u_0}-\frac{c_1}{c_0}\right)\phi_1'-\frac{U'}{u_0}\phi_1\\
&\qquad-\left\{2\frac{c_2}{c_0}+\left(\frac{U}{u_0}-\frac{c_1}{c_0}\right)^2\right\}\phi_0'+\frac{U'}{u_0}\left(\frac{U}{u_0}-\frac{c_1}{c_0}\right)\phi_0\,, \quad (y=0)
\end{aligned}\right\} \tag{3.18a, b, c}$$

where

$$g_r=g+\frac{\sigma k^2}{\rho}\,. \tag{3.19}$$

The bottom condition (3.14) becomes

$$\phi_0=\phi_1=\phi_2=\cdots=0\,. \quad (y=-d) \tag{3.20}$$

The zeroth-order solution for (3.17a), (3.18a) and (3.20) leads to

$$\phi_0=A\sinh k(y+d), \tag{3.21}$$

$$c_0^2=(g_r/k)\tanh kd\,, \tag{3.22}$$

where A is an arbitrary constant. The first- and second-order solutions ϕ_1 and ϕ_2 may be written in the integral forms

$$\phi_1=-\frac{1}{ku_0}\int_{-d}^{y}U''(\xi)\phi_0(\xi)\sinh k(y-\xi)d\xi\,, \tag{3.23}$$

$$\phi_2=-\frac{1}{ku_0}\int_{-d}^{y}U''(\xi)\left[\phi_1(\xi)-\phi_0(\xi)\left(\frac{c_1}{c_0}-\frac{U}{u_0}\right)\right]\sinh k(y-\xi)d\xi\,. \tag{3.24}$$

As a matter of course, Eqs. (3.23) and (3.24) are just the same as the forms of ϕ_1 and ϕ_2 found by Kato (1972) in a somewhat different way following Hunt (1955). However, calculations of (3.23) and (3.24) for the present logarithmic profile (3.1) are much more complicated than the previous parabolic profile, because $U''(y)\neq$ const. for (3.1).

Upon substitution of (3.1) and (3.21) into (3.23) and evaluation of the integrals, ϕ_1 is obtained as follows:

$$\phi_1(y)=-\frac{AU_r}{2u_0k}[I_1(y)-I_2(y)]\,, \tag{3.25}$$

where

$$I_1(y)\equiv\int_{-d}^{y}\frac{\cosh k(y+d)}{(z_0-\xi)^2}d\xi=\cosh k(y+d)\left[\frac{1}{z_0-y}-\frac{1}{z_0+d}\right], \tag{3.26}$$

$$I_2(y)\equiv\int_{-d}^{y}\frac{\cosh k(2\xi+d-y)}{(z_0-\xi)^2}d\xi$$

$$\equiv\cosh k(2z_0+d-y)\cdot I_{2c}(y)+\sinh k(2z_0+d-y)\cdot I_{2s}(y)\,, \tag{3.27a}$$

$$\left.\begin{aligned}I_{2c}(y)&=2k\left[-\frac{\cosh 2k(y-z_0)}{2k(y-z_0)}-\frac{\cosh y_2}{y_2}+\mathrm{Shi}\,\{2k(y-z_0)\}+\mathrm{Shi}\,(y_2)\right],\\ I_{2s}(y)&=2k\left[-\frac{\sinh 2k(y-z_0)}{2k(y-z_0)}+\frac{\sinh y_2}{y_2}+\mathrm{Chi}\,\{2k(y-z_0)\}-\mathrm{Chi}\,(y_2)\right],\end{aligned}\right\} \tag{3.27b, c}$$

and further

$$\left.\begin{aligned}\mathrm{Shi}\,(x)&=x+\frac{x^3}{3\cdot 3!}+\frac{x^5}{5\cdot 5!}+\frac{x^7}{7\cdot 7!}+\cdots,\\ \mathrm{Chi}\,(x)&=\log|x|+\frac{x^2}{2\cdot 2!}+\frac{x^4}{4\cdot 4!}+\frac{x^6}{6\cdot 6!}+\cdots,\end{aligned}\right\} \tag{3.28}$$

$$\left.\begin{aligned}y_1&=2kz_0\,,\\ y_2&=2k(d+z_0)\,,\end{aligned}\right\} \tag{3.29}$$

y_1 appears in the next equation. Substituting above results in (3.18b) gives

$$\frac{c_1}{c_0}=1+\frac{U_r}{u_0}\left(\frac{Q}{2k\sinh 2kd}-\frac{\delta}{2kz_0}\tanh kd\right), \tag{3.30}$$

where

$$Q=2k\left[\frac{\cosh 2kd}{y_1}-\frac{1}{y_2}+\sinh y_2\{\mathrm{Chi}\,(y_1)-\mathrm{Chi}\,(y_2)\}\right.$$

$$\left.+\cosh y_2\{\mathrm{Shi}\,(y_2)-\mathrm{Shi}\,(y_1)\}\right]-\frac{d}{z_0(d+z_0)}, \tag{3.31}$$

$$\delta=1-\frac{z_0b}{U_r}\,. \tag{3.32}$$

Hence, the wave speed to the first-order approximation is given by

$$c=c_0+\varepsilon c_1=c_0\left[1+\varepsilon\frac{c_1}{c_0}\right]. \tag{3.33}$$

In the evaluation of the second-order solution (3.24), we write

$$\beta=1-\frac{c_1}{c_0}, \tag{3.34}$$

and

$$\beta_1=\beta+\frac{U_r}{u_0}\ln z_0. \tag{3.35}$$

Using (3.34), the surface condition (3.18c) is rewritten in the form

$$\phi_2'-\left(\frac{g_r}{c_0^2}\right)\phi_2=2\beta\phi_1'-\frac{U'}{u_0}\phi_1-\left(2\frac{c_2}{c_0}+\beta^2\right)\phi_0'+\frac{U'}{u_0}\beta\phi_0', \quad (y=0) \tag{3.36}$$

Since the terms on the right hand side of Eq. (3.36) are already known except c_2/c_0, the expression of c_2/c_0 will be obtained if only the left hand side of (3.36) is evaluated. Some process of the evaluation will be shown in Appendix, and the final form becomes

$$\phi_2'(0)-\left(\frac{g_r}{c_0^2}\right)\phi_2(0)=-\frac{A}{\sinh kd}\left[\frac{U_r\beta_1}{2u_0}Q+\frac{kU_r^2}{u_0^2}(G_a+G_b+G_{II})+\frac{bU_r}{2u_0^2}G_{III}\right], \tag{3.37}$$

where

$$G_{III}=1-\cosh 2kd-(y_1\sinh y_2+\cosh y_2)(\mathrm{Chi}\,y_1-\mathrm{Chi}\,y_2)$$
$$+(y_1\cosh y_2+\sinh y_2)(\mathrm{Shi}\,y_1-\mathrm{Shi}\,y_2)+\log(y_1/y_2). \tag{3.38}$$

$$(G_a+G_b+G_{II})=H_1-H_2+H_3+H_4+H_5, \tag{3.39}$$

$$\left.\begin{aligned}
H_1&=\sinh y_2\{-\log y_1\cdot\mathrm{CSY}(y_1)+\mathrm{Fch}(y_1)\}+\cosh y_2\{\log y_1\cdot\mathrm{SCY}(y_1)-\mathrm{Fsh}(y_1)\}\\
&\quad-\frac{m}{y_1}+\frac{\log y_1}{y_1}-m\cosh y_2\cdot\mathrm{SCY}(y_1)+m\sinh y_2\cdot\mathrm{CSY}(y_1),\\
H_2&=\sinh y_2\{-\log y_2\cdot\mathrm{CSY}(y_2)+\mathrm{Fch}(y_2)\}+\cosh y_2\{\log y_2\cdot\mathrm{SCY}(y_2)-\mathrm{Fsh}(y_2)\}\\
&\quad-\frac{m}{y_2}+\frac{\log y_2}{y_2}-m\cosh y_2\cdot\mathrm{SCY}(y_2)+m\sinh y_2\cdot\mathrm{SCY}(y_2),\\
H_3&=\frac{1}{y_1}\{\sinh y_2(\mathrm{Shi}\,y_2-\mathrm{Shi}\,y_1)-\cosh y_2(\mathrm{Chi}\,y_2-\mathrm{Chi}\,y_1)\},\\
H_4&=\frac{1}{y_1}\{\sinh y_1(\mathrm{Shi}\,y_1-\mathrm{Shi}\,y_2)-\cosh y_1(\mathrm{Chi}\,y_1-\mathrm{Chi}\,y_2)\},\\
H_5&=\mathrm{Chi}\,y_1\cdot\mathrm{Shi}\,y_1-2\cdot\mathrm{CKS}(y_1)+\mathrm{Shi}\,y_2\cdot\mathrm{Chi}\,y_1-\mathrm{Chi}\,y_2\cdot\mathrm{Shi}\,y_1\\
&\quad+2\cdot\mathrm{CKS}(y_2)-\mathrm{Chi}\,y_2\cdot\mathrm{Shi}\,y_2.
\end{aligned}\right\} \tag{3.40}$$

$$m=\ln(2k), \tag{3.41}$$

$$\left.\begin{aligned}
\mathrm{SCY}(x)&\equiv\mathrm{Shi}(x)-\frac{\cosh x}{x},\\
\mathrm{CSY}(x)&\equiv\mathrm{Chi}(x)-\frac{\sinh x}{x},
\end{aligned}\right\} \tag{3.42}$$

$$\left.\begin{aligned}\mathrm{Fsh}(x)&=\int\frac{\mathrm{Shi}(x)}{x}dx=x+\frac{x^3}{3^2\cdot 3!}+\frac{x^5}{5^2\cdot 5!}+\frac{x^7}{7^2\cdot 7!}+\cdots,\\ \mathrm{Fch}(x)&=\int\frac{\mathrm{Chi}(x)}{x}dx=\frac{(\log|x|)^2}{2}+\frac{x^2}{2^2\cdot 2!}+\frac{x^4}{4^2\cdot 4!}+\frac{x^6}{6^2\cdot 6!}+\cdots,\end{aligned}\right\}\quad (3.43)$$

$$\mathrm{CKS}(x)=\int_0^x\frac{\cosh x\,\mathrm{Shi}(x)}{x}dx, \quad (3.44)$$

$$\begin{aligned}&=x+\left(\frac{1}{2!}+\frac{1}{3\cdot 3!}\right)\frac{x^3}{3}+\left(\frac{1}{4!}+\frac{1}{2!}\cdot\frac{1}{3\cdot 3!}+\frac{1}{5\cdot 5!}\right)\frac{x^5}{5}+\cdots\\ &+\left\{\frac{1}{(n-1)!}+\frac{1}{(n-3)!}\times\frac{1}{3\cdot 3!}+\frac{1}{(n-5)!}\times\frac{1}{5\cdot 5!}+\cdots\right.\\ &\left.+\frac{1}{2!}\times\frac{1}{(n-2)\cdot(n-2)!}+\frac{1}{n\cdot n!}\right\}\frac{x^n}{n}+\cdots\end{aligned}\quad (3.45)$$

Some remarks will be made later concerning the functions $\mathrm{Fsh}(x)$, $\mathrm{Fch}(x)$, $\mathrm{CKS}(x)$.

By using (3.37), c_2/c_0 is obtained from (3.36) in the form

$$\frac{c_2}{c_0}=E_1+E_2+E_3+E_4, \quad (3.46)$$

where

$$\left.\begin{aligned}E_1&=\frac{1}{\sinh 2kd}\left[\frac{s\beta_1}{2k}Q+s^2(G_a+G_b+G_{\mathrm{II}})+\frac{bU_r}{2ku_0^2}G_{\mathrm{III}}\right],\\ E_2&=-\frac{\beta s}{2k}\left[\frac{d\tanh kd}{z_0(z_0+d)}+\frac{1}{\cosh kd}\{G_1\cosh k(2z_0+d)+G_2\sinh k(2z_0+d)\}\right],\\ E_3&=\frac{s^2\delta}{4k^2z_0}\left[\frac{d}{z_0(z_0+d)}-\frac{1}{\cosh kd}\{G_1\sinh k(2z_0+d)+G_2\cosh k(2z_0+d)\}\right],\\ E_4&=\frac{s\delta\beta}{2kz_0}\tanh kd-\frac{1}{2}\beta^2,\end{aligned}\right\}\quad (3.47)$$

and further

$$s=\frac{U_r}{u_0}, \quad (3.48)$$

$$\left.\begin{aligned}G_1&=2k[\mathrm{CSY}(y_1)-\mathrm{CSY}(y_2)],\\ G_2&=2k[\mathrm{SCY}(y_2)-\mathrm{SCY}(y_1)].\end{aligned}\right\}\quad (3.49)$$

After all, the wave speed to the second-order approximation is given by

$$c=c_0+\varepsilon c_1+\varepsilon^2c_2=c_0\left[1+\varepsilon\frac{c_1}{c_0}+\varepsilon^2\frac{c_2}{c_0}\right], \quad (3.50)$$

where $\varepsilon=u_0/c_0$. In order to express effect of surface velocity u_0 on the wave speed, we introduce a parameter G_l such as

$$c=c_0+u_0G_l, \quad (3.51)$$

that is, from (3.50)

$$G_l=\frac{c_1}{c_0}+\varepsilon\frac{c_2}{c_0}. \quad (3.52)$$

4. Numerical results and discussions

The numerical computations of c_1/c_0 and c_2/c_0 are carried out mainly by using the values of the above-mentioned functions, such as Shi(x), Chi(x), Fsh(x), Fch(x) and CKS(x), for y_1 and y_2 in Eq. (3.29). In Appendix A, some functional values of those functions are listed in Table A-1 and their behaviors for small values of x are shown in Fig. A-1. The values of y_1 and y_2 for $z_r=2.0\times10^{-4}$ (say, $z_0=0.01$ cm for $d=50$ cm) are shown in Table 2. As seen from this table the functional values for fairly large values of y_2 are needed for the numerical computations. From this origin arise the troubles of reduction of significant figures in the course of the machine computations. In order to avoid the serious errors due to the figure-dropping for large values of y_2 the following approximations were seeked and used.

Table 2 Values of y_1 and y_2 (for $z_r=2.0\times10^{-4}$)

L/d	y_1	y_2
0.1	0.02513	125.69
0.2	0.012566	62.844
0.3	0.008378	41.896
0.4	0.006283	31.422
0.6	0.004189	20.948
0.8	0.003142	15.711
1.0	0.002513	12.569
1.2	0.002094	10.474
1.6	0.001571	7.8556
2.0	0.001257	6.2844

(a) If we write

$$\mathrm{SMC}(x)\equiv\mathrm{Shi}(x)-\mathrm{Chi}(x), \quad (4.1)$$

then, as $x\to\infty$

$$\mathrm{SMC}(x)\to\gamma(=0.57721566490) \quad (4.2)$$

where γ is called Euler's constant. Practically (4.2) gives the accuracy more than 10 figures for $x\geqq18$.

(b) Let

$$\mathrm{FDh}(x)\equiv\mathrm{Fsh}(x)-\mathrm{Fch}(x), \quad (4.3)$$

then

$$\mathrm{FDh}(x)\to\gamma\log_e x+0.989055995 \quad (4.4)$$

(4.4) gives the accuracy more than 9 figures for $x\geqq15.0$.

(c) Let

$$\mathrm{DIF}(x)\equiv2\cdot\mathrm{CKS}(x)-\mathrm{Shi}(x)\cdot\mathrm{Chi}(x) \quad (4.5)$$

then for large values of x

$$\mathrm{DIF}(x)\to\gamma\,\mathrm{Shi}(x),\ \text{or}\ \gamma\,\mathrm{Chi}(x) \quad (4.6)$$

The approximation (4.6) gives the accuracy more than 8 figures for $x\geqq25.0$, and more than 6 figures for $x\geqq18.0$.

So far we have used dimensional quantities. If, however, we use a non-dimensional parameter z_r $(=z_0/d)$ in place of z_0, then c_1/c_0 and c_2/c_0 can be evaluated as functions of only kd and do not depend on the magnitude of u_0 (This never denys the correlation between z_0 and u_0). The evaluated values of c_1/c_0 and c_2/c_0 for a typical value of $z_r=2.0\times10^{-4}$ are shown at the second and third columns in Table 3, and those values for the several cases with different values of z_r are shown in Table A-2 in Appendix A together with the values of $\bar{c}$, which is given by

$$\bar{c}=c_0/(gd)^{1/2} \quad (4.7)$$

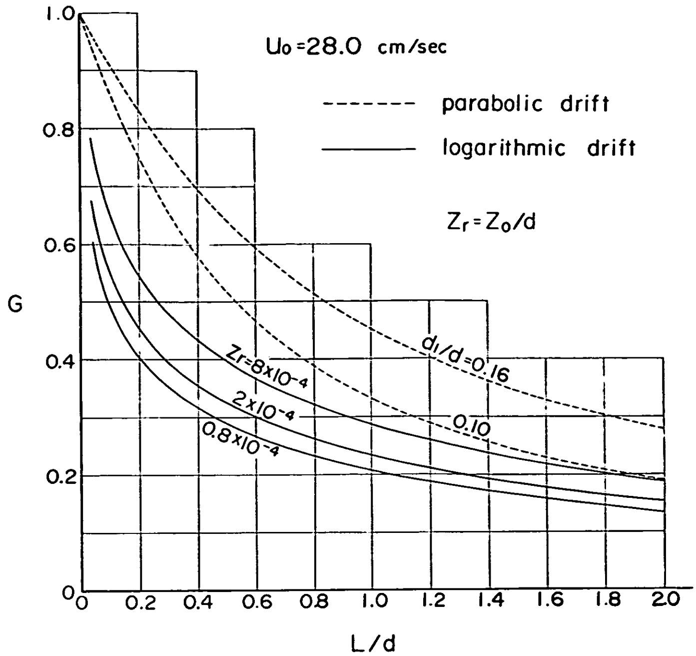

Fig. 4. Curves of G.

For a particular case it is found that the smaller L/d are, the larger c_1/c_0 are and the smaller c_2/c_0 contrarily. As mentioned earlier, for the drift current which we encounter in the laboratory the parameter $\varepsilon(=u_0/c_0)$ is not so small as usually used in the perturbation method. Since ε is largest for waves with the smallest length, there is an inverse trend between the magnitudes of c_2/c_1 and ε. Let us inspect the convergence of the wave speeds given by (3.50). For that purpose the evaluated values $\varepsilon c_1/c_0$, $\varepsilon^2 c_2/c_0$, c and G_l for the cases of $u_0=15.0$ and 28.0 cm/sec with $z_0=0.01$ cm and $d=50$ cm ($z_r=2\times10^{-4}$) are also shown in Table 3. As a matter of course the convergence is better for $u_0=15.0$ cm/sec than $u_0=28.0$ cm/sec. However, even in the latter case where ε is considerablly large for short waves, the second-order contribution $\varepsilon^2 c_2/c_0$ to the wave speed is much smaller than the first-order one $\varepsilon c_1/c_0$ for the shown wavelength range. This fact presumably suggests that the parameter ε may have been overestimated, because, as seen from Fig. 3, the velocity scale representative of the drift current of this type may be not the surface velocity u_0 but much smaller one.

The fact that the second-order term is very small was also found by Kato (1972) for the case of parabolic current profile, which is shown in Fig. 5. In that case the wave speeds were also calculated by using the method of expanding the solutions ϕ into power series (cf. Appendix C), verify-

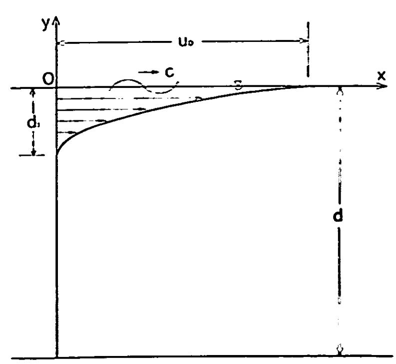

Fig. 5. Parabolic profile (from Kato[2]).

Table 3 Numerical results for profile (2.4) with $z_r=2.0\times10^{-4}$

L/d	c_1/c_0	c_2/c_0	L (cm)	c_0 (cm/sec)	$u_0=15.0$ cm/sec				$u_0=28.0$ cm/sec			
					$\varepsilon c_1/c_0$	$\varepsilon^2 c_2/c_0$	c (cm/sec)	G_l	$\varepsilon c_1/c_0$	$\varepsilon^2 c_2/c_0$	c (cm/sec)	G_l
0.1	0.53121	0.01439	5	29.501	0.27009	0.00372	37.579	0.5385	0.50418	0.01296	44.758	0.5449
0.2	0.43772	0.01776	10	40.062	0.16389	0.00249	46.728	0.4444	0.30593	0.00868	52.666	0.4501
0.3	0.38242	0.02056	15	48.680	0.11784	0.00195	54.511	0.3888	0.21996	0.00680	59.719	0.3942
0.4	0.34323	0.02324	20	56.054	0.09185	0.00166	61.296	0.3495	0.17145	0.00580	65.990	0.3548
0.5	0.31301	0.02590	25	62.589	0.07502	0.00149	67.377	0.3192	0.14003	0.00518	71.678	0.3246
0.6	0.28851	0.02858	30	68.514	0.06316	0.00137	72.936	0.2948	0.11791	0.00477	76.920	0.3002
0.7	0.26799	0.03128	35	73.973	0.05434	0.00129	78.087	0.2743	0.10144	0.00448	81.808	0.2798
0.8	0.25039	0.03402	40	79.058	0.04751	0.00122	82.911	0.2568	0.08868	0.00427	86.406	0.2624
0.9	0.23501	0.03677	45	83.838	0.04205	0.00118	87.462	0.2416	0.07849	0.00410	90.762	0.2473
1.0	0.22141	0.03956	50	88.361	0.03759	0.00114	91.782	0.2281	0.07016	0.00397	94.911	0.2339
1.2	0.19827	0.04523	60	96.775	0.03073	0.00109	99.854	0.2053	0.05736	0.00379	102.692	0.2114
1.4	0.17916	0.05098	70	104.507	0.02572	0.00105	107.304	0.1865	0.04800	0.00366	109.906	0.1928
1.6	0.16302	0.05681	80	111.686	0.02189	0.00102	114.246	0.1706	0.04087	0.00357	116.649	0.1773
1.8	0.14914	0.06268	90	118.391	0.01890	0.00101	120.747	0.1571	0.03527	0.00351	122.982	0.1640
2.0	0.13705	0.06858	100	124.674	0.01649	0.00099	126.853	0.1453	0.03078	0.00346	128.942	0.1524

Table 4 Numerical results for profile (2.3) with $z_r=2.0\times10^{-4}$

L/d	c_1/c_0	c_2/c_0	L (cm)	c_0 (cm/sec)	$u_0=15.0$ cm/sec				$u_0=28.0$ cm/sec			
					$\varepsilon c_1/c_0$	$\varepsilon^2 c_2/c_0$	c (cm/sec)	G_l	$\varepsilon c_1/c_0$	$\varepsilon^2 c_2/c_0$	c (cm/sec)	G_l
0.1	0.52960	0.01309	5	29.501	0.26927	0.00338	37.545	0.5363	0.50264	0.01179	44.678	0.5420
0.2	0.43449	0.01457	10	40.062	0.16268	0.00204	46.661	0.4399	0.30367	0.00712	52.513	0.4447
0.3	0.37757	0.01524	15	48.680	0.11634	0.00145	54.414	0.3823	0.21717	0.00504	59.497	0.3863
0.4	0.33677	0.01564	20	56.054	0.09012	0.00112	61.168	0.3410	0.16822	0.00390	65.702	0.3446
0.5	0.30494	0.01591	25	62.589	0.07308	0.00091	67.220	0.3087	0.13642	0.00318	71.327	0.3121
0.6	0.27882	0.01611	30	68.514	0.06104	0.00077	72.750	0.2823	0.11395	0.00269	76.506	0.2854
0.7	0.25668	0.01626	35	73.973	0.05205	0.00067	77.872	0.2600	0.09716	0.00233	81.332	0.2628
0.8	0.23746	0.01639	40	79.058	0.04506	0.00059	82.667	0.2406	0.08410	0.00206	85.870	0.2433
0.9	0.22046	0.01647	45	83.838	0.03944	0.00053	87.189	0.2234	0.07363	0.00184	90.165	0.2260
1.0	0.20525	0.01655	50	88.361	0.03484	0.00048	91.481	0.2081	0.06504	0.00166	94.254	0.2105
1.2	0.17888	0.01669	60	96.775	0.02773	0.00040	99.497	0.1815	0.05176	0.00140	101.918	0.1837
1.4	0.15655	0.01680	70	104.507	0.02247	0.00035	106.891	0.1590	0.04194	0.00121	109.016	0.1610
1.6	0.13719	0.01689	80	111.686	0.01843	0.00030	113.778	0.1395	0.03439	0.00106	115.646	0.1414
1.8	0.12011	0.01700	90	118.391	0.01522	0.00027	120.225	0.1223	0.02841	0.00095	121.867	0.1241
2.0	0.10485	0.01712	100	124.674	0.01262	0.00025	126.277	0.1069	0.02355	0.00086	127.717	0.1087

Table 5 Numerical results for the parabolic profile (1)

$u_0=15.0$ cm/sec, $d_1=5.0$ cm, $d=50$ cm

L/d	$(c_1/c_0)_p$	$(c_2/c_0)_p$	Perturbation method					S.E. Method		α
			ε	$\varepsilon(c_1/c_0)_p$	$\varepsilon^2(c_2/c_0)_p$	c_p (cm/sec)	G_p	c_s (cm/sec)	G_s	
0.1	0.85351	0.00903	0.5085	0.43397	0.00234	42.3730	0.85810	42.37442	0.85820	0.000051
0.2	0.73226	0.02488	0.3744	0.27417	0.00349	51.1855	0.74157	51.19290	0.74207	0.000187
0.4	0.55727	0.04688	0.2676	0.14912	0.00336	64.6012	0.56981	64.62123	0.57115	0.000359
0.6	0.44487	0.05462	0.2189	0.09740	0.00262	75.3669	0.45683	75.39085	0.45842	0.000348
0.8	0.36883	0.05563	0.1897	0.06998	0.00200	84.7488	0.37938	84.77188	0.38092	0.000292
1.2	0.27392	0.05135	0.1550	0.04246	0.00123	101.0028	0.28188	101.02073	0.28308	0.000186
1.6	0.21752	0.04573	0.1343	0.02921	0.00082	115.0407	0.22366	115.05420	0.22456	0.000120
2.0	0.18028	0.04089	0.1203	0.02169	0.00059	127.4517	0.18520	127.46205	0.18589	0.000083

Table 6 Numerical results for the parabolic profile (2)

$u_0=28.0$ cm/sec, $d_1=5.0$ cm, $d=50$ cm

L/d	L (cm)	c_0 (cm/sec)	Perturbation method					S.E. method		α
			ε	$\varepsilon(c_1/c_0)_p$	$\varepsilon^2(c_2/c_0)_p$	c_p (cm/sec)	G_p	c_s (cm/sec)	G_s	
0.1	5	29.501	0.9491	0.81007	0.00814	53.640	0.86209	53.6477	0.86237	0.00027
0.2	10	40.062	0.6989	0.51179	0.01215	61.052	0.74965	61.0957	0.75121	0.00109
0.4	20	56.054	0.4995	0.27836	0.01170	72.313	0.58069	72.440	0.58520	0.00225
0.6	30	68.514	0.4087	0.18181	0.00912	81.596	0.46719	81.754	0.47282	0.00230
0.8	40	79.058	0.3542	0.13063	0.00698	89.937	0.38853	90.092	0.39408	0.00197
1.2	60	96.775	0.2893	0.07925	0.00430	104.860	0.28878	104.984	0.29320	0.00128
1.6	80	111.686	0.2507	0.05453	0.00287	118.097	0.22899	118.191	0.23233	0.00084
2.0	100	124.674	0.2246	0.04049	0.00206	129.979	0.18946	130.051	0.19203	0.00058

ing the results from the perturbation method. The results newly obtained for the parabolic drift current with $d_1/d=0.10$ ($d=50$ cm), $u_0=15.0$ and 28.0 cm/sec are shown in Table 5 and 6. Assuming that the difference between c_s and c_p is attributed to the error in the perturbation method, we write

$$c_s=c_0\left[1+\varepsilon\left(\frac{c_1}{c_0}\right)_p+\varepsilon^2\left(\frac{c_2}{c_0}\right)_p+\alpha\right], \tag{4.8}$$

that is,

$$\alpha=(c_s-c_p)/c_0\,. \tag{4.9}$$

Then the evaluated values of α are found to be much smaller than $\varepsilon^2(c_2/c_0)_p$, especially for short waves, as shown at the last columns in both tables. From this fact the validity of the present perturbation method would be assured.

Based upon these considerations, the obtained wave speeds to the second-order approximation for the present logarithmic profile may be regarded as being accurate sufficiently. It might further be possible to neglect the second-order term in (3.50) for most practical use.

The results for the profile (2.3), which are obtained simply by putting $b=0$ in the final equations relevant to Eq. (3.50), in the same cases as those in Table 3 are shown in Table 4. By comparing contents of the two tables it can be seen that the difference of the wave speeds for the two profiles is unexpectedly small, especially for the waves of small length. The evaluated values of c_1/c_0 and c_2/c_0 for the profile (2.3) are also shown in Table A-3 in Appendix A.

In Fig. 4 are shown the curves of G_l obtained from (3.52) for three different profiles (2.4) with $u_0=28.0$ cm/sec and also corresponding curves of G_p for two parabolic profiles (cf. Fig. 5). It is found from this figure that the parabolic profile for $d_1/d=0.16$, which was selected as a representative one in the previous paper[2], gives fairly larger wave speeds, especially for short waves, than the present logarithmic profile with z_r of about 2×10^{-4}.

5. Summary and conclusions

In this paper an attempt has been made towards a better expression for the effect of drift current on the wave speeds. Main results and findings are as follows:

(1) A proposed logarithmic distribution (2.3) or (2.4) is well applicable to the observed drift current profiles.

(2) Using the perturbation method, the wave speed solution for the proposed drift current profile has been obtained to the second-order in the form of (3.50) where c_1/c_0 and c_2/c_0 can be evaluated independently of the surface velocity u_0.

(3) The second-order contributions to the wave speeds were found to be very small even when the perturbation parameter ε ($=u_0/c_0$) is relatively large.

(4) The modification of the velocity profile near the bottom for a return flow has little effect on the wave speed. On the other hand, the present logarithmic profile gives fairly smaller wave speeds than the parabolic profile which was assumed previously. This indicates that the form of the drift current profile close to the water surface is very important in determining the wave speeds.

(5) Great care was needed against the reduction of significant figures in the

course of machine computations, and asymptotic forms of the special functions which appear in the calculation were seeked and used.

The numerical computations have been carried out by the use of a digital computer TOSBAC-3400 at the Computer Center of the Port and Harbour Research Institute.

References

1) Hidy, G.M. & Plate, E.J. (1966) Wind action on water standing in a laboratory channel, with Appendix by Lilly, D.K., J. Fluid Mech., **26**, 651-687.
2) Kato, H. (1972) The calculation of wave speed for a parabolic drift current, Proc. 19th Conf. Coastal Eng. in Japan, 113-118, (in Japanese).
3) Shemdin, O.H. (1972) Wind-generated current and phase speed of wind waves, J. Phys. Oceanog., **2**, 411-419.
4) Dobroklonsky, S.S. & Lesnikov, B.M. (1972) A study of near surface layer of drift currents in laboratory conditions, Izv. Acad. Sci., Atm. Oceanic Physics, 8, 1177-1187.
5) Mizuno, S. & Mitsuyasu, H. (1973a) Experimental studies on the decay of waves by adverse wind (2), Proc. 20th Conf. Coastal Eng. in Japan, 457-461, (in Japanese).
6) Mizuno, S. & Mitsuyasu, H. (1973b) Effects of adverse wind on the phase velocity of mechanically generated water waves, Rep. Res. Inst. Appl. Mech., Kyushu Univ., Vol. XXI, No. 68, 33-52.
7) Kato, H. & Tsuruya, H. (1974) On phase velocities of spectral components of wind waves, Proc. 21st Conf. Coastal Eng. in Japan, 255-259, (in Japanese).
8) Keulegan, G.H. (1951) Wind tides in small closed channels, J. Res. Nat. Bur. Stand., **46**, 358-381.
9) Plate, E.J., Chang, P.C. & Hidy, G.M. (1969) Experiments on the generation of small water waves by wind, J. Fluid Mech., **35**, 625-656.
10) Wu, J. (1968) Laboratory studies of wind-wave interactions, J. Fluid Mech., **34**, 91-111.
11) Baines, W.D. & Knapp, D.J. (1965) Wind driven water currents, Proc. ASCE, **91**, HY2, 205-221.
12) Banner, M.L. & Phillips, O.M. (1973) On small scale breaking waves, Tech. Report, Chesapeake Bay Inst. The Johns Hopkins Univ. No. 82.
13) Hunt, N.J. (1955) Gravity waves in flowing water, Proc. Roy. Soc, A, **231**, 496-504.

(Received 30 September 1974)

List of Symbols

a : wave amplitude
A : arbitrary constant for ϕ_0
A_1, B_1 : arbitrary constants, cf. Eq. (2.1)
b : coefficient of the linear term in Eq. (2.4)
c_0 : phase velocity for no current
c : phase velocity of the waves in a current
c_1, c_2 : first- and second-order wave speeds, cf. Eq. (3.16)
$\bar{c}$: non-dimensional wave speed, $=c_0/(gd)^{1/2}$
c_p : wave speed obtained from the perturbation method for the parabolic drift
c_s : wave speed obtained from the series expansion method for the parabolic drift
d : depth of water
d_1 : depth of the parabolic drift, cf. Fig. 5
$E_1 \sim E_4$: terms in the expression for c_2/c_0, cf. Eqs. (3.46) and (3.47)
g : acceleration of gravity
g_r : $g+(\sigma k^2/\rho)$
G_1, G_2 : cf. Eq. (3.49)
G_a, G_b, G_{II}: terms appearing in the calculation of the left hand side of Eq. (3.36) cf. Eqs. (3.37) and (3.39)
G_{III} : term similar to G_a, G_b and G_{II}, but originating from the linear term in Eq. (2.4), cf. Eqs. (3.37) and (3.38)
G_l : $(c-c_0)/u_0$ for logarithmic drift
G_p : $(c_p-c_0)/u_0$ for parabolic drift
G_s : $(c_s-c_0)/u_0$ for parabolic drift
$H_1 \sim H_5$: terms in the expression for $(G_a+G_b+G_{II})$, cf. Eq. (3.39)
k : wavenumber $(=2\pi/L)$
L : wavelength
m : $\ln(2k)$
p : pressure in water
Q : cf. Eq. (3.31)
s : U_r/u_0
u_0 : surface drift current velocity, $=U(0)$
U : drift current velocity
U_r : arbitrary constant in the logarithmic distribution, Eqs. (2.3) or (2.4)
u, v : x- and y-components of velocity due to the wave motion
V : average wind velocity
V_∞ : free stream wind velocity
x : horizontal axis in the direction of the current
y : vertical axis measured upward from the water surface
y_1 : $2kz_0$
y_2 : $2k(d+z_0)$
z : depth from the water surface
z_0 : arbitrary constant in the logarithmic distribution, Eqs. (2.3) or (2.4)
z_{0_w} : roughness height, cf. Eq. (2.2)
z_r : non-dimensional quantity for z_0 $(=z_0/d)$

α : $(c_s - c_p)/c_0$, cf. Eq. (4.8)
β : $1-(c_1/c_0)$
β_1 : cf. Eq. (3.35)
γ : Euler's constant ($=0.57721566490\cdots$)
δ : correction factor due to the linear term in Eq. (2.4), cf. Eq. (3.32)
ε : perturbation parameter ($=u_0/c_0$)
η : water surface displacement
ν : kinematic viscosity
ξ : integration variable
ρ : water density
σ : surface tension
τ_0 : mean tangential wind stress at the water surface
ϕ : function of y only (y-dependent factor of stream function)
ϕ_0, ϕ_1, ϕ_2: zeroth-, first- and second-order solutions of ϕ, cf. Eq. (3.15)
Ψ : stream function, $=\phi(y)e^{ik(x-ct)}$
$I_1(y)$: term in the expression for $\phi_1(y)$, cf. Eqs. (3.25) and (3.26)
$I_2(y)$: term in the expression for $\phi_1(y)$, cf. Eqs. (3.25) and (3.27a)
$I_{2c}(y)$, $I_{2s}(y)$: terms in the expression for $I_2(y)$, cf. Eqs. (3.27a, b, c)
CKS(x) : special function defined by Eqs. (3.44) and (3.45)
Fsh(x), Fch(x): special functions defined by Eq. (3.43)
Shi x, Chi x: hyperbolic sine integral and cosine integral, cf. Eq. (3.28)
SCY(x) : Shi $x-(\cosh x/x)$
CSY(x) : Chi $x-(\sinh x/x)$

Appendix A

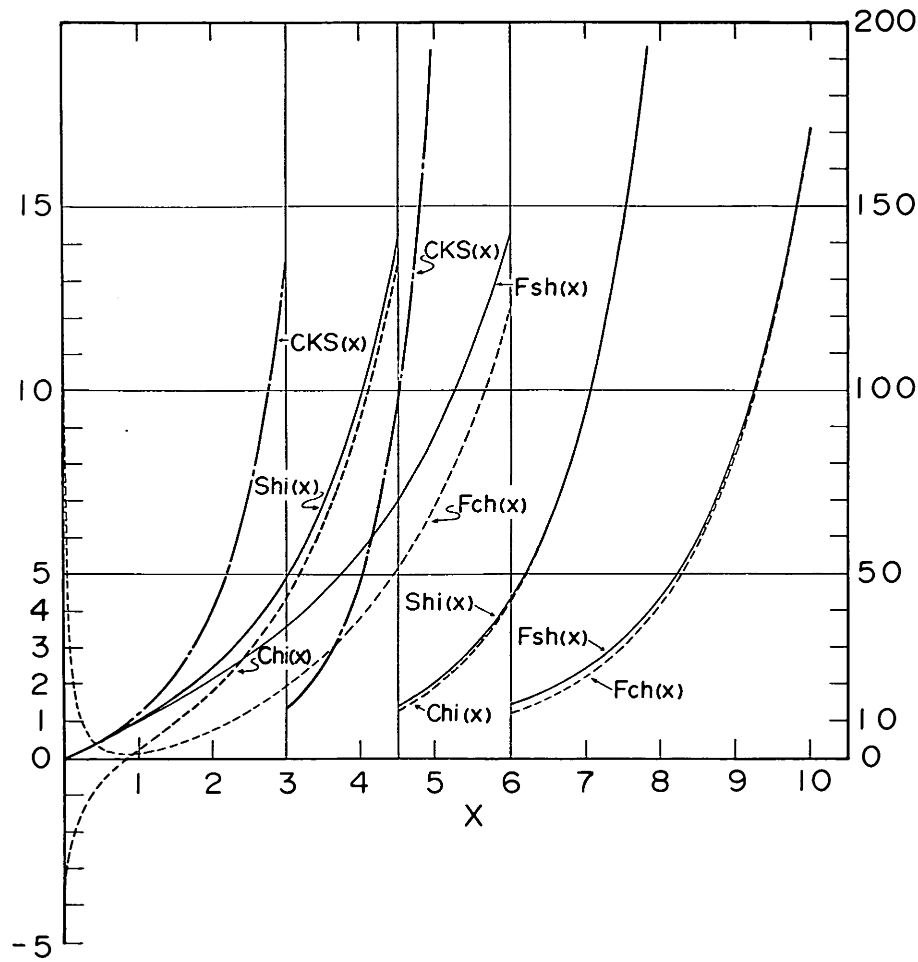

Fig. A-1. The variations of the special functions for $0 \leqq x \leqq 10$.

Table A-1 Table of the Special Functions

x	Shi x	Chi x	SMC(x)	CKS(x)	Fsh(x)	Fch(x)	FDh(x)
0.1	0.1000556 E 00	−0.2300084 E 01	0.2400140 E 01	0.1001853 E 00	0.1000185 E 00	0.2652199 E 01	−0.2552181 E 01
0.2	0.2004450 E 00	−0.1599421 E 01	0.1799866 E 01	0.2014860 E 00	0.2001483 E 00	0.1300149 E 01	−0.1100001 E 01
0.3	0.3015041 E 00	−0.1181388 E 01	0.1482892 E 01	0.3050347 E 00	0.3005008 E 00	0.7360464 E 00	−0.4355456 E 00
0.4	0.4035727 E 00	−0.8760231 E 00	0.1279596 E 01	0.4119986 E 00	0.4011886 E 00	0.4398612 E 00	−0.3867257 E -01
0.5	0.5069967 E 00	−0.6299925 E 00	0.1136989 E 01	0.5235977 E 00	0.5023253 E 00	0.2716399 E 00	0.2306854 E 00
0.6	0.6121304 E 00	−0.4194648 E 00	0.1031595 E 01	0.6411244 E 00	0.6040260 E 00	0.1758107 E 00	0.4282153 E 00
0.7	0.7193380 E 00	−0.2316465 E 00	0.9509845 E 00	0.7659634 E 00	0.7064082 E 00	0.1254883 E 00	0.5809199 E 00
0.8	0.8289966 E 00	−0.5881568 E -01	0.8878122 E 00	0.8996147 E 00	0.8095916 E 00	0.1059734 E 00	0.7036182 E 00
0.9	0.9414978 E 00	0.1040982 E 00	0.8373996 E 00	0.1043718 E 01	0.9136988 E 00	0.1085297 E 00	0.8051691 E 00
1.0	0.1057251 E 01	0.2606513 E 00	0.7965996 E 00	0.1200081 E 01	0.1018856 E 01	0.1276431 E 00	0.8912128 E 00
2.0	0.2501567 E 01	0.1875451 E 01	0.6261162 E 00	0.4031711 E 01	0.2159351 E 01	0.7844644 E 00	0.1374887 E 01
3.0	0.4973440 E 01	0.4383176 E 01	0.5902640 E 00	0.1338998 E 02	0.3590564 E 01	0.1970250 E 01	0.1620313 E 01
4.0	0.9817327 E 01	0.9236332 E 01	0.5809950 E 00	0.4927369 E 02	0.5602716 E 01	0.3814144 E 01	0.1788572 E 01
5.0	0.2009321 E 02	0.1951485 E 02	0.5783640 E 00	0.2029873 E 03	0.8750657 E 01	0.6832781 E 01	0.1917876 E 01
6.0	0.4299506 E 02	0.4241749 E 02	0.5775757 E 00	0.9254283 E 03	0.1415769 E 02	0.1213445 E 02	0.2023241 E 01
7.0	0.9575243 E 02	0.9517510 E 02	0.5773311 E 00	0.4585419 E 04	0.2418194 E 02	0.2206968 E 02	0.2112253 E 01
8.0	0.2201900 E 03	0.2196127 E 03	0.5772533 E 00	0.2424298 E 05	0.4390840 E 02	0.4171906 E 02	0.2189338 E 01
9.0	0.5189392 E 03	0.5183619 E 03	0.5772281 E 00	0.1346501 E 06	0.8454191 E 02	0.8228458 E 02	0.2257327 E 01
10.0	0.1246114 E 04	0.1245537 E 04	0.5772198 E 00	0.7764018 E 06	0.1712244 E 03	0.1689062 E 03	0.2318144 E 01
11.0	0.3035703 E 04	0.3035126 E 04	0.5772170 E 00	0.4607748 E 07	0.3612512 E 03	0.3588781 E 03	0.2373159 E 01
12.0	0.7479766 E 04	0.7479189 E 04	0.5772161 E 00	0.2797345 E 08	0.7869494 E 03	0.7845261 E 03	0.2423383 E 01
13.0	0.1859884 E 05	0.1859827 E 05	0.5772157 E 00	0.1729585 E 09	0.1757510 E 04	0.1755040 E 04	0.2469585 E 01
14.0	0.4659626 E 05	0.4659568 E 05	0.5772157 E 00	0.1085606 E 10	0.4002767 E 04	0.4000255 E 04	0.2512361 E 01
15.0	0.1174779 E 06	0.1174773 E 06	0.5772157 E 00	0.6900532 E 10	0.9260984 E 04	0.9258432 E 04	0.2552185 E 01
16.0	0.2977805 E 06	0.2977799 E 06	0.5772157 E 00	0.4433661 E 11	0.2170522 E 05	0.2170263 E 05	0.2589438 E 01
17.0	0.7583189 E 06	0.7583184 E 06	0.5772157 E 00	0.2875238 E 12	0.5142489 E 05	0.5142227 E 05	0.2624431 E 01
18.0	0.1938952 E 07	0.1938952 E 07	0.5772157 E 00	0.1879768 E 13	0.1229688 E 06	0.1229661 E 06	0.2657424 E 01
19.0	0.4975454 E 07	0.4975453 E 07	0.5772157 E 00	0.1237757 E 14	0.2964087 E 06	0.2964060 E 06	0.2688632 E 01
20.0	0.1280783 E 08	0.1280783 E 08	0.5772157 E 00	0.8202021 E 14	0.7195029 E 06	0.7195002 E 06	0.2718240 E 01
21.0	0.3306359 E 08	0.3306359 E 08	0.5772157 E 00	0.5466006 E 15	0.1757399 E 07	0.1757396 E 07	0.2746402 E 01
22.0	0.8557234 E 08	0.8557234 E 08	0.5772157 E 00	0.3661312 E 16	0.4316332 E 07	0.4316329 E 07	0.2773254 E 01
23.0	0.2219832 E 09	0.2219832 E 09	0.5772157 E 00	0.2463827 E 17	0.1065424 E 08	0.1065424 E 08	0.2798912 E 01
24.0	0.5770577 E 09	0.5770577 E 09	0.5772157 E 00	0.1664978 E 18	0.2641719 E 08	0.2641719 E 08	0.2823478 E 01
25.0	0.1502975 E 10	0.1502975 E 10	0.5772157 E 00	0.1129468 E 19	0.6577019 E 08	0.6577019 E 08	0.2847042 E 01
30.0	0.1844866 E 12	0.1844866 E 12	0.5772157 E 00	0.1701765 E 23	0.6616770 E 10	0.6616770 E 10	0.2952280 E 01
35.0	0.2334528 E 14	0.2334528 E 14	0.5772157 E 00	0.2725009 E 27	0.7095537 E 12	0.7095537 E 12	0.3041259 E 01
40.0	0.3019859 E 16	0.3019859 E 16	0.5772157 E 00	0.4559775 E 31	0.7964736 E 14	0.7964736 E 14	0.3118335 E 01
45.0	0.3971958 E 18	0.3971958 E 18	0.5772157 E 00	0.7888225 E 35	0.9253060 E 16	0.9253060 E 16	0.3186321 E 01
50.0	0.5292818 E 20	0.5292818 E 20	0.5772157 E 00	0.1400696 E 40	0.1104187 E 19	0.1104187 E 19	0.3247137 E 01
55.0	0.7127343 E 22	0.7127343 E 22	0.5772157 E 00	0.2539951 E 44	0.1346290 E 21	0.1346290 E 21	0.3302151 E 01
60.0	0.9680911 E 24	0.9680911 E 24	0.5772157 E 00	0.4685998 E 48	0.1670679 E 23	0.1670679 E 23	0.3352376 E 01
65.0	0.1324466 E 27	0.1324466 E 27	0.5772157 E 00	0.8769455 E 52	0.2103982 E 25	0.2103982 E 25	0.3398578 E 01
70.0	0.1823176 E 29	0.1823176 E 29	0.5772157 E 00	0.1650774 E 57	0.2682947 E 27	0.2682947 E 27	0.3441354 E 01

Table A-2 Evaluated values of c_1/c_0 and c_2/c_0 for profile (2.4)

L/d	$\bar{c}$	$z_r=8.0\times10^{-4}$		$z_r=2.0\times10^{-4}$		$z_r=8.0\times10^{-5}$		$z_r=2.0\times10^{-5}$	
		c_1/c_0	c_2/c_0	c_1/c_0	c_2/c_0	c_1/c_0	c_2/c_0	c_1/c_0	c_2/c_0
0.1	0.13327	0.63281	0.01518	0.53121	0.01439	0.47523	0.01295	0.40680	0.01057
0.2	0.18098	0.52842	0.02074	0.43772	0.01776	0.38995	0.01549	0.33285	0.01246
0.3	0.21991	0.46446	0.02493	0.38242	0.02056	0.34006	0.01780	0.28993	0.01436
0.4	0.25323	0.41838	0.02867	0.34323	0.02324	0.30490	0.02010	0.25977	0.01630
0.5	0.28275	0.38248	0.03224	0.31301	0.02590	0.27786	0.02241	0.23662	0.01828
0.6	0.30951	0.35317	0.03573	0.28851	0.02858	0.25598	0.02477	0.21792	0.02030
0.7	0.33418	0.32849	0.03921	0.26779	0.03128	0.23768	0.02715	0.20230	0.02236
0.8	0.35715	0.30725	0.04269	0.25039	0.03402	0.22202	0.02960	0.18901	0.02453
0.9	0.37874	0.28864	0.04618	0.23501	0.03677	0.20831	0.03203	0.17723	0.02654
1.0	0.39917	0.27214	0.04969	0.22141	0.03956	0.19621	0.03451	0.16692	0.02869
1.1	0.41861	0.25735	0.05322	0.20924	0.04238	0.18540	0.03701	0.15771	0.03084
1.2	0.43718	0.24398	0.05678	0.19827	0.04523	0.17565	0.03953	0.14940	0.03301
1.3	0.45499	0.23181	0.06036	0.18829	0.04809	0.16679	0.04208	0.14185	0.03520
1.4	0.47211	0.22067	0.06396	0.17916	0.05098	0.15869	0.04464	0.13495	0.03741
1.5	0.48862	0.21041	0.06758	0.17077	0.05388	0.15124	0.04722	0.12861	0.03962
1.6	0.50455	0.20092	0.07122	0.16302	0.05681	0.14436	0.04982	0.12276	0.04185
1.7	0.51994	0.19212	0.07488	0.15583	0.05974	0.13799	0.05242	0.11733	0.04408
1.8	0.53484	0.18392	0.07855	0.14914	0.06268	0.13205	0.05503	0.11228	0.04632
1.9	0.54926	0.17625	0.08222	0.14289	0.06563	0.12652	0.05764	0.10756	0.04856
2.0	0.56322	0.16908	0.08590	0.13705	0.06857	0.12133	0.06026	0.10315	0.05078
		$U_r/u_0=0.18365$		$U_r/u_0=0.14650$		$U_r/u_0=0.12918$		$U_r/u_0=0.10957$	
		$b/u_0=0.00509$		$b/u_0=0.00405$		$b/u_0=0.00358$		$b/u_0=0.00304$	

Table A-3 Evaluated values of c_1/c_0 and c_2/c_0 for profile (2.3)

L/d	$\bar{c}$	$z_r=8.0\times10^{-4}$		$z_r=2.0\times10^{-4}$		$z_r=8.0\times10^{-5}$		$z_r=2.0\times10^{-5}$	
		c_1/c_0	c_2/c_0	c_1/c_0	c_2/c_0	c_1/c_0	c_2/c_0	c_1/c_0	c_2/c_0
0.1	0.13327	0.63078	0.01398	0.52960	0.01309	0.47380	0.01163	0.40559	0.00926
0.2	0.18098	0.52437	0.01756	0.43449	0.01457	0.38710	0.01237	0.33044	0.00950
0.3	0.21991	0.45839	0.01940	0.37757	0.01524	0.33579	0.01269	0.28630	0.00959
0.4	0.25323	0.41028	0.02057	0.33677	0.01564	0.29920	0.01287	0.25493	0.00965
0.5	0.28275	0.37236	0.02139	0.30494	0.01591	0.27073	0.01300	0.23058	0.00968
0.6	0.30951	0.34103	0.02201	0.27882	0.01611	0.24743	0.01308	0.21067	0.00971
0.7	0.33418	0.31433	0.02250	0.25668	0.01626	0.22770	0.01315	0.19384	0.00974
0.8	0.35715	0.29106	0.02290	0.23746	0.01639	0.21062	0.01323	0.17934	0.00983
0.9	0.37874	0.27043	0.02323	0.22046	0.01647	0.19549	0.01325	0.16636	0.00974
1.0	0.39917	0.25190	0.02350	0.20525	0.01655	0.18197	0.01329	0.15483	0.00977
1.1	0.41861	0.23509	0.02374	0.19147	0.01663	0.16973	0.01331	0.14441	0.00977
1.2	0.43718	0.21970	0.02396	0.17888	0.01669	0.15855	0.01334	0.13489	0.00978
1.3	0.45499	0.20551	0.02414	0.16729	0.01674	0.14827	0.01336	0.12614	0.00979
1.4	0.47211	0.19234	0.02432	0.15655	0.01680	0.13875	0.01339	0.11803	0.00980
1.5	0.48862	0.18007	0.02448	0.14655	0.01684	0.12988	0.01341	0.11049	0.00981
1.6	0.50455	0.16857	0.02463	0.13719	0.01689	0.12158	0.01344	0.10343	0.00982
1.7	0.51994	0.15776	0.02477	0.12840	0.01695	0.11379	0.01346	0.09681	0.00984
1.8	0.53484	0.14756	0.02492	0.12011	0.01700	0.10645	0.01350	0.09056	0.00986
1.9	0.54926	0.13791	0.02507	0.11228	0.01706	0.09951	0.01353	0.08466	0.00988
2.0	0.56322	0.12875	0.02522	0.10485	0.01712	0.09294	0.01357	0.07907	0.00990
		$U_r/u_0=0.18365$		$U_r/u_0=0.14650$		$U_r/u_0=0.12918$		$U_r/u_0=0.10957$	
		$b/u_0=0.00509$		$b/u_0=0.00406$		$b/u_0=0.00358$		$b/u_0=0.00304$	

Appendix B Reduction of Eq. (3.37)

$\phi_2(y)$ can be written, from (3.24) and (3.1), in the form

$$\phi_2(y)=\beta_1\phi_1(y)-\frac{1}{ku_0}[\phi_{2_{\rm I}}(y)-\phi_{2_{\rm II}}(y)-\phi_{2_{\rm III}}(y)], \tag{B.1}$$

where

$$\phi_{2_{\rm I}}(y)=\int_{-d}^{y}U''(\xi)\phi_1(\xi)\sinh k(y-\xi)d\xi, \tag{B.2}$$

$$\phi_{2_{\rm II}}(y)=\frac{U_r}{u_0}\int_{-d}^{y}U''(\xi)\phi_0(\xi)\ln(z_0-\xi)\sinh k(y-\xi)d\xi, \tag{B.3}$$

$$\phi_{2_{\rm III}}(y)=\frac{b}{u_0}\int_{-d}^{y}U''(\xi)\xi\phi_0(\xi)\sinh k(y-\xi)d\xi. \tag{B.4}$$

Hence, the left hand side of Eq. (3.36) becomes

$$\phi_2'(0)-\left(\frac{g_r}{c_0^2}\right)\phi_2(0)=\beta_1\phi_1'(0)-\beta_1 kR\phi_1(0)-\frac{1}{ku_0}[\phi_{2_{\rm I}}'(0)-kR\phi_{2_{\rm I}}(0)]$$
$$+\frac{1}{ku_0}[\phi_{2_{\rm II}}'(0)-kR\phi_{2_{\rm II}}(0)]+\frac{1}{ku_0}[\phi_{2_{\rm III}}'(0)-kR\phi_{2_{\rm III}}(0)], \tag{B.5}$$

where

$$R=\coth kd.$$

The first term on the right hand side of (B.5) becomes

$$\beta_1\phi_1'(0)-\beta kR\phi_1(0)=-\frac{AU_r}{2u_0\sinh kd}Q. \tag{B.6}$$

The three bracketed terms on the right hand side are calculated in the following ways. The first bracketed terms are

$$\phi_{2_{\rm I}}'(0)-kR\phi_{2_{\rm I}}(0)=\frac{Ak^2U_r^2}{u_0\sinh kd}(G_a+G_b), \tag{B.7}$$

where

$$G_a=-\frac{\sinh kd}{2k^2}\left[\int_{-d}^{0}\frac{I_1(\xi)\cosh k\xi}{(z_0-\xi)^2}d\xi+R\int_{-d}^{0}\frac{I_1(\xi)\sinh k\xi}{(z_0-\xi)^2}d\xi\right], \tag{B.8}$$

$$G_b=\frac{\sinh kd}{2k^2}\left[\int_{-d}^{0}\frac{I_2(\xi)\cosh k\xi}{(z_0-\xi)^2}d\xi+R\int_{-d}^{0}\frac{I_2(\xi)\sinh k\xi}{(z_0-\xi)^2}d\xi\right], \tag{B.9}$$

The function CKS(x), given by (3.44), comes out from the calculation of G_b. The second bracketed terms are

$$\phi_{2_{\rm II}}'(0)-kR\phi_{2_{\rm II}}(0)=\frac{Ak^2U_r^2}{u_0\sinh kd}G_{\rm II}, \tag{B.10}$$

where

$$G_{\rm II}=\frac{1}{2k}\int_{-d}^{0}\frac{\ln(z_0-\xi)}{(z_0-\xi)^2}\sinh^2 k(\xi+d)d\xi. \tag{B.11}$$

The functions Fsh(x) and Fch(x), given by (3.43), come out from $G_{\rm II}$. The third bracketed terms are

$$\phi'_{2\rm III}(0)-kR\phi_{2\rm III}(0)=\frac{-AkbU_r}{2u_0\sinh kd}G_{\rm III}, \tag{B.12}$$

where

$$G_{\rm III}=-2\int_{-d}^{0}\frac{\xi\sinh^2 k(\xi+d)}{(z_0-\xi)^2}d\xi, \tag{B.13}$$

Eq. (B.5) with (B.6), (B.7), (B.10) and (B.12) gives Eq. (3.37) in the text. Eqs. (3.38)~(3.40) are obtained from (B.13), (B.8), (B.9) and (B.11).

Appendix C Method of series expansion for the parabolic drift

The method of series expansion used in the calculation for the parabolic drift is as follows:

The velocity distribution of Fig. 5 is

$$\left.\begin{array}{ll} U(y)=\dfrac{u_0}{d_1^2}(y+d_1)^2, & (\text{I: } 0\geqq y\geqq -d_1) \\ U(y)=0. & (\text{II: } -d_1\geqq y\geqq -d) \end{array}\right\} \tag{C.1}$$

The equation for ϕ is

$$(U-c)(\phi''-k^2\phi)-U''\phi=0. \tag{C.2}$$

We need two separate solutions $\phi_{\rm I}$ and $\phi_{\rm II}$ for the depth range I and II, respectively, and the two solutions must give the equal values of p and v at the boundary $y=-d_1$. Concerning the waves satisfying $c>u_0$, the equation (C.2) has no singular point for $0\geqq y\geqq -d_1$. Therefore a power series solution exists in the neighborhood of an arbitrary point $y=y_1$ in the range I. Here we seek such two solutions ϕ_a and ϕ_b for the depth $y_1=0$ and $y_1=-d_1$. ϕ_a and ϕ_b are combined at the depth $y=-d_1/2$ with two conditions for p and v, and ϕ_b is also combined with $\phi_{\rm II}$ similarly at the depth $y=-d_1$. Then the surface condiaion (3.13) applied to ϕ_a leads to the equation from which c is obtained.

ϕ_a and ϕ_b are put in the forms

$$\phi_a=a_0+a_1y+a_2y^2+a_3y^3+\cdots, \tag{C.3}$$

$$\phi_b=b_0+b_1(y+d_1)+b_2(y+d_1)^2+b_3(y+d_1)^3+\cdots. \tag{C.4}$$

Substitution of (C.1) in (C.2) leads to

$$(y^2+2d_1y+D)\phi''-k^2y^2\phi-2d_1k^2y\phi-(Dk^2+2)\phi=0, \tag{C.5}$$

where

$$D=d_1^2-\frac{d_1^2}{u_0}c=d_1^2\beta_0, \tag{C.6}$$

$$\beta_0=\left(1-\frac{c}{u_0}\right). \tag{C.7}$$

Upon substituting (C.3) into (C.5) a_n are obtained successively, and ϕ_a takes the following form:

$$\phi_a = a_0(1+P_2y^2+P_3y^3+P_4y^4+\cdots)+a_1(y+Q_3y^3+Q_4y^4+Q_5y^5+\cdots), \quad \text{(C.8)}$$

where

$$\left.\begin{aligned}
P_2 &= \frac{1}{2D}(Dk^2+2),\\
P_3 &= -\frac{2}{3}\frac{d_1^2}{D^2},\\
Q_3 &= \frac{1}{6D}(Dk^2+2),\\
P_4 &= \frac{1}{24D^2}\left[(Dk^2+2)^2-4-\frac{16d_1^2}{D}\right],\\
Q_4 &= -\frac{1}{3}\frac{d_1}{D^2}.
\end{aligned}\right\} \quad \text{(C.9)}$$

If we put $P_1=Q_2=0$ and $Q_1=1$ the coefficients P_n, Q_n for $n\geqq 5$ can be obtained numerically from the following relations:

$$\begin{aligned}
P_n &= \frac{1}{n(n-1)D}[-2(n-1)(n-2)d_1P_{n-1}-(n-2)(n-3)P_{n-2}\\
&\quad +(Dk^2+2)P_{n-2}+2d_1k^2P_{n-3}+k^2P_{n-4}], \quad \text{(C·10)}
\end{aligned}$$

$$\begin{aligned}
Q_n &= \frac{1}{n(n-1)D}[-2(n-1)(n-2)d_1Q_{n-1}-(n-2)(n-3)Q_{n-2}\\
&\quad +(Dk^2+2)Q_{n-2}+2d_1k^2Q_{n-3}+k^2Q_{n-4}]. \quad \text{(C·11)}
\end{aligned}$$

If we show, for reference, P_n and Q_n up to $n=7$

$$\left.\begin{aligned}
P_5 &= \frac{1}{5}\left(-\frac{2}{3}\frac{d_1k^2}{D^2}+\frac{2}{3}\frac{d_1}{D^3}-\frac{4d_1^3}{D^4}\right),\\
Q_5 &= \frac{1}{20}\left(\frac{k^4}{6}+\frac{2}{3}\frac{k^2}{D}-\frac{4}{3}\frac{1}{D^2}+8\frac{d_1^2}{D^3}\right),\\
P_6 &= \frac{1}{30}\left(\frac{k^6}{24}+\frac{k^4}{4D}-\frac{2}{3}\frac{k^2}{D^2}+\frac{14}{3}\frac{d_1^2k^2}{D^3}-12\frac{d_1^2}{D^4}+32\frac{d_1^4}{D^5}\right),\\
Q_6 &= \frac{1}{30}\left(-\frac{d_1k^2}{D^2}+6\frac{d_1}{D^3}-16\frac{d_1^3}{D^4}\right),\\
P_7 &= \frac{1}{42}\left(-\frac{3}{10}\frac{d_1k^4}{D^2}+\frac{16}{5}\frac{d_1k^2}{D^3}-\frac{44}{5}\frac{d_1^3k^2}{D^4}-\frac{12}{5}\frac{d_1}{D^4}+\frac{192}{5}\frac{d_1^3}{D^5}-64\frac{d_1^5}{D^6}\right),\\
Q_7 &= \frac{1}{42}\left(\frac{k^6}{120}+\frac{1}{20}\frac{k^4}{D}-\frac{1}{3}\frac{k^2}{D^2}+\frac{26}{15}\frac{d_1^2k^2}{D^3}+\frac{6}{5}\frac{1}{D^3}-\frac{96}{5}\frac{d_1^2}{D^4}+32\frac{d_1^4}{D^5}\right).
\end{aligned}\right\}$$

(C.12)

Similarly ϕ_b takes the form

$$\begin{aligned}
\phi_b &= b_0[1+H_2(y+d_1)^2+H_4(y+d_1)^4+\cdots]\\
&\quad +b_1[(y+d_1)+H_3(y+d_1)^3+H_5(y+d_1)^5+\cdots], \quad \text{(C.13)}
\end{aligned}$$

where

$$\left.\begin{aligned} H_2&=\frac{1}{2S}(k^2S-2),\\ H_3&=\frac{1}{6S}(k^2S-2), \end{aligned}\right\} \tag{C.14}$$

$$S=\frac{d_1^2}{u_0}c=d_1^2(1-\beta_0). \tag{C.15}$$

By putting $H_0=H_1=1$, H_n for $n\geqq 4$ can be obtained from

$$H_n=\frac{1}{n(n-1)S}[(k^2S-2)H_{n-2}+(n-2)(n-3)H_{n-2}-k^2H_{n-4}], \tag{C.16}$$

If we show H_n up to $n=7$

$$\left.\begin{aligned} H_4&=\frac{k^2}{24S}(k^2S-4),\\ H_5&=\frac{1}{120S^2}(k^4S^2-4k^2S-8),\\ H_6&=\frac{1}{720}\frac{k^2}{S^2}(k^4S^2-6k^2S-16),\\ H_7&=\frac{1}{5040}\frac{1}{S^3}(k^6S^3-6k^4S^2-40k^2S-144). \end{aligned}\right\} \tag{C.17}$$

The ratio b_1/b_0 is determined from the conditions for p and v at $y=-d_1$:

$$R\equiv\frac{b_1}{b_0}=k\coth k(d-d_1). \tag{C.18}$$

The ratio a_1/a_0 ($\equiv F_3$) is obtained in the form

$$F_3\equiv\frac{a_1}{a_0}=-\frac{X_1(W_3+RW_4)-X_3(W_1+RW_2)}{X_2(W_3+RW_4)-X_4(W_1+RW_2)}, \tag{C.19}$$

where, by putting $d_1/2=e$,

$$\left.\begin{aligned} X_1&=1+P_2e^2-P_3e^3+P_4e^4-P_5e^5+\cdots\\ X_2&=-e-Q_3e^3+Q_4e^4-Q_5e^5+\cdots\\ X_3&=-2P_2e+3P_3e^2-4P_4e^3+5P_5e^4-\cdots\\ X_4&=1+3Q_3e^2-4Q_4e^3+5Q_5e^4-\cdots \end{aligned}\right\} \tag{C.20}$$

$$\left.\begin{aligned} W_1&=1+H_2e^2+H_4e^4+H_6e^6+\cdots\\ W_2&=e+H_3e^3+H_5e^5+H_7e^7+\cdots\\ W_3&=2H_2e+4H_4e^3+6H_6e^5+\cdots\\ W_4&=1+3H_3e^2+5H_5e^4+7H_7e^6+\cdots \end{aligned}\right\} \tag{C.21}$$

Substituting (C.7), (C.8) and (C.19) into Eq. (3.13) in the text leads to the final equation for β_0:

$$\beta_0\left(\beta_0F_3-\frac{2}{d_1}\right)=\frac{g_r}{u_0^2} \tag{C.22}$$

since F_3 is the function of k and β_0, Eq. (C.22) determines β_0 proper to the problem and c is obtained from (C.7), that is,

$$c=u_0(1-\beta_0)\,. \tag{C.23}$$

For the present problem a negative root ($\beta_0<0$) is what we seek, since $c>u_0>0$. Although the convergence of the series in (C.19) is very slow for the waves of small length, complete convergence could be obtained by raising the power n as high as needed by means of (C.10), (C.11) and (C.16). However, it was found in the present computations shown in Table 6 that the convergence is greatly improved by combining ϕ_a and ϕ_b at the depth $y=-d_1/3$ instead of $y=-d_1/2$.

港湾技術研究所報告　第13巻 第4号

1974・12

編集兼発行人　運輸省港湾技術研究所

発 行 所　運輸省港湾技術研究所
横須賀市長瀬3丁目1番1号

印 刷 所　啓 文 堂 松 本 印 刷
東京都新宿区戸塚町 1－458－14